Mechanical, Rheological and Computational Study of PVP/PANI with Additives

Taghizadeh, Mohammad Taghi*+; Nasirianfar, Saeed***

Department of Physical Chemistry, Faculty of Chemistry, University of Tabriz, P.O. Box 51666-14766 Tabriz, I.R. IRAN

ABSTRACT: *Polyvinylpyrrolidone/polyaniline emeraldine salt (PVP/PANI) with additives (TiO_2, ZnO, NaCl, and Na_2SO_4) was synthesized via oxidative in situ polymerization. Because of using PVP/PANI as a protective membrane layer and its applications in an electrical device, we investigated the mechanical and rheological properties of PVP/PANI and other composites in order to spread the application of this composite. Mechanical properties of PVP/PANI, PVP/PANI/TiO_2, PVP/PANI/ZnO, PVP/PANI/NaCl, and PVP/PANI/Na_2SO_4 films were studied using the tensile test to obtain tensile strength, elongation at the break, and Young's modulus. To gain some comprehensive information, rheometry tests were implemented and the storage modulus, loss modulus, and complex viscosity were measured. Interactions between additives and polymers were investigated by NBO analysis. Results from experimental and computational methods show that TiO_2, ZnO, and Na_2SO_4 increase the interactions in the polymer matrix, respectively. However, NaCl weakens these interactions.*

KEYWORDS: *NBO analysis; Polyvinylpyrrolidone/Polyaniline; Rheology; Tensile.*

INTRODUCTION

Polyaniline (PANI) has desirable properties such as low monomer cost, simple polymerization methods, desired environmental-thermal stability, and suitable optical, electrochemical, and chemical properties [1-3]. PANI composite was used in purification and removal process [4]. However, some serious problems exist in the application of PANI such as insolubility, non-processability, and poor mechanical properties, which restricted the development of its applications. To overcome these problems, composites of PANI and suitable materials were synthesized [5-8].

Polyvinylpyrrolidone (PVP) is a water-soluble polymer that is used as a pore-forming agent for membranes [3]. PVP can be thermally crosslinked and makes the composites stable, resulting in an increase in the mechanical strength of the composite [9]. PVP improved properties such as hardness, crystallinity, solubility, and thermal resistance of composites. Furthermore, it helps to bond the composite with a solid surface to make a thin film with uniform thickness [10]. Pyrrolidone group of PVP makes complexes with many inorganic salts and modifies their dispersion [9]. Because of these properties, PVP has been used as a matrix for the composites.

In the oxidative polymerization of aniline in aqueous acidic solution, PVP acted as a stabilizer [11].

** To whom correspondence should be addressed.*
+ E-mail: mttaghizadeh@tabrizu.ac.ir
1021-9986/2020/1/281-296 16/$/6.06

Polyaniline and polyvinylpyrrolidone blend are important materials because of a combination of electrical properties of PANI as conducting polymer and good mechanical properties of PVP as a conventional insulating polymer. In PVP/PANI, hydrogen bonding between the N-hydrogen of PANI and the carbonyl group of PVP are developed. Hydrogen bonding in PVP/PANI causes a high degree of dispersion of the PANI in this blend [1, 11].

These polymers have been used in ultrafiltration membranes for drug purification, wastewater treatment, reverse osmosis membranes, a nanofiltration membrane, and gas separation membranes. The ability of this blend to sense NO_2, NO, NH_3, H_2, ethanol, methanol, and acetone were studied. PVP/PANI showed good results for NH_3 gas sensing. Furthermore, this blend has acted as a protective layer for the prevention of corrosion and provided a hospitable matrix for biological materials [12-14]. PVP/PANI nanocomposite significantly improved membrane surface hydrophilicity, water wettability, and pore hydrophilicity [2].

To improve the mechanical properties of polymers (polymers with poor mechanical properties), their composite and blend with other polymers were prepared [15].

Insoluble and infusible nature of PANI led to bad processability, which makes it difficult to study this polymer rheologically [16]. PANI is grown and dispersed within the PVP matrix as a water-soluble support polymer in a nanoscopic form. Interactions between two polymers (mainly hydrogen bonding between PVP and PANI) affected the rheological properties within the system. The interaction between PVP and PANI increased rigidity and so the storage modulus. Steady and dynamic rheological properties of the PVP/PANI dispersion/colloid along with pure PVP and PANI solutions (in DMSO) were studied by Gangopadhyay [17].

The mechanical properties of polymer composites are affected by several factors: intrinsic properties of components, production process, interactions between the components, the state of dispersion, the size of the filler, and the degree of crystallinity of the matrix [18-20]. In these composites, the flexibility of PVP chain and less flexibility of the shorter macromolecular chain of PANI give the moderate flexibility to the nanocomposite. The pure PVP/PANI film was rigid and brittle and difficult to handle [6, 7], so PVP/PANI composite with additives was synthesized. Inorganic nanofillers are added to polymer composites to modify their mechanical properties [18].

In this regard, titanium dioxide (TiO_2) has several applications because of properties such as low toxicity, biological and chemical inertness, stability toward photocorrosion, low costs, and suitable redox potential for photodegrading pollutants. A coordinate bond was formed between titanium and nitrogen in the amine group of the PANI and hydrogen bonding was established between them in the form of NH-O-Ti [21, 22]. PANI/TiO_2 was used as an anticorrosive coating [23]. Zinc oxide (ZnO) has good chemical stability and biocompatibility. This nanocomposite was investigated for the use as a gas sensor [24]. Sodium chloride (NaCl) was used for DNA separation and in pharmaceutical applications. NaCl had a positive impact on nanoclay retention in the nanocomposite. NaCl acted as a weak crazing and embrittling agent [25-27]. It has been reported that some chloride salts increase the water content of polymer blends and restrained the recrystallization of the polymer. Furthermore, inorganic counterions (Cl^-, SO_4^{2-}) produce films that are brittle and rough [5, 28].

Sodium sulfate (Na_2SO_4) is a non-toxic inorganic salt. Sodium sulfate has many commercial applications because of its unique heat storage properties. The addition of sodium sulfate to a polymer increases conductivity and the crystallite area of the polymer composites. It modifies mechanical properties and facilitates the uniform preparation of films [29, 30]. The importance of hydrogen bonding in the viscoelastic properties of polymer blends was emphasized by researchers. The difference in the viscoelastic response of the solutions indicates the structural difference between different samples [17]. The Natural Bond Orbital (NBO) analysis is a useful tool to study delocalization of electron density from occupied NBOs (as a donor) to properly unoccupied NBOs (as acceptor) between two chemical species. To investigate interactions between the components (especially hydrogen bonding between them), NBO analysis was used.

Regarding the electrical, membrane, and protective layer applications of PVP/PANI, studies of mechanical and rheological properties of PVP/PANI and other composites are important. These composites are obtained from a combination of PVP/PANI and TiO_2, ZnO,

Na_2SO_4, and NaCl. In this regard, studying the mechanical and rheological properties is effective in the spread of PVP/PANI applications. In the present work, PVP/PANI, PVP/PANI/TiO_2, PVP/PANI/ZnO, PVP/PANI/NaCl, and PVP/PANI/Na_2SO_4 were synthesized *via* oxidative in situ polymerization method. The mechanical, rheological, and computational methods were used to investigate the structures, properties, and interactions between constituent components.

EXPERIMENTAL SECTION

Materials

Aniline, ammonium persulfate, anhydrous ethanol, HCl, NaCl, and ZnO were obtained from Merck. Na_2SO_4 and polyvinylpyrrolidone (M_r = 360000) were purchased from Fluka. Titanium (IV) Oxide (TiO_2) was purchased from TECNAN. All materials were used without further purification. Water was used after two distillations as Double Distilled Water (DDW).

Synthesis of PVP/PANI

PVP/PANI was synthesized via chemical oxidative in situ polymerization, with the ammonium persulfate (APS) as an oxidant according to instructions in the literature [13, 31]. To prepare this blend, 18 g of PVP and 0.05 g of Aniline has been dissolved in 50 mL aqueous HCl solution (pH = 1). Aniline was added to PVP solution and a final solution put on a bath at 0-2℃ with constant magnetic stirring for 1 h. Then, 0.115 g of APS was dissolved in 100 mL DDW and added to the solution as dropwise. The mixture was kept at 0-2℃ with constant magnetic stirring for 4 h and then was kept in the refrigerator for 20 h [13]. The final products were thoroughly washed with DDW and anhydrous ethanol several times. Then, the composite was filmed and dried at 80℃ in an air oven for 4 h [6]. These films were used in the tensile test. A similar procedure was employed for the synthesis of PVP/PANI/TiO_2, PVP/PANI/ZnO, PVP/PANI/NaCl, and PVP/PANI/Na_2SO_4 composite films. TiO_2, ZnO, NaCl, and Na_2SO_4 were added to the solution of the aniline for in situ polymerization, separately.

Tensile test

The tensile strength (stress) is defined as the maximum stress (σ_{max}) sustained by the film. Elongation at the break (strain) was defined as the ratio of the change in the length (ΔL) of the sample to its original length (L). Young's modulus was calculated from the initial slope of the tensile curves [32, 33]. The plots are relatively linear over this range. The tensile strength (σ_y), Young's modulus (E), and elongation at break (ε_b) of PVP/PANI, PVP/PANI/TiO_2, PVP/PANI/ZnO, PVP/PANI/Na_2SO_4, and PVP/PANI/NaCl were studied using an Instron (model 6025) with Crosshead speed 5 mm/min under ASTM D638 standard. The specimens were prepared according to ASTM D638 Type-I standard. The thickness of the sample was 7 mm (0.28 in.) [34]. All measurements were done with three repetitions for each data point at room temperature.

Rheological properties

To describe the flow and deformation of maters, rheology study was applied. Rheology is a useful tool to survey the structural properties and molecular interactions of materials [17]. The rheological properties of the blends and their components influence their morphology, which controls the mechanical properties of the composites [17, 35, 36]. Especially, the storage modulus is sensitive to the particles' dispersion and interfacial interaction in the polymer matrix. So, it is used as a criterion to evaluate the interfacial interaction between the particles and polymers. Indeed, the storage modulus is related to the elastically stores energy while the loss modulus is due to the energy that is lost as heat [37]. Viscosity is one of the important properties of fluids. This structurally sensitive resistance against the flow results from cohesion and molecular momentum exchange between fluid layers when it flows. Viscosity has an intrinsic relation with the microstructure of a fluid [38].

The storage modulus (G′) is a measure of the material stiffness (rigidity) that represents the solid-like component of the rheological behavior [5, 39]. In other words, the storage modulus indicates the capability of a material to store mechanical energy without disintegration, suggesting that the higher the storage modulus, the stiffer and stronger the material is [18, 39]. The elastic response of materials is represented by the storage modulus; however, the loss modulus shows the viscous response [32]. The complex viscosity (η*) shows the viscous resistance of the solution, as:

$$\eta^* = \sqrt{\left(\frac{G'}{\omega}\right)^2 + \left(\frac{G''}{\omega}\right)^2} \quad (1)$$

where G', G", and ω are the storage modulus, loss modulus, and angular frequency, respectively [17, 35].

The storage modulus (G'), loss modulus (G"), and complex viscosity (η*) of the PVP/PANI, PVP/PANI/TiO_2, PVP/PANI/ZnO, PVP/PANI/Na_2SO_4, and PVP/PANI/NaCl were measured as a function of angular frequency (ω) at 25℃. These parameters were determined using an MCR 300 rheometer (Anton Paar GmbH, Graz, Austria) with oscillatory frequency sweeps from 0.1 to 100 rad/s. This determination was carried out at a constant deformation (1% strain amplitude) within the linear viscoelastic region, in which the moduli are independent of the applied strain [17]. Approximately, 12 mL of any sample solution was used for each measurement.

COMPUTATIONAL DETAILS

NBO analysis was applied in order to study the interaction between the components of the blends. All computations were implemented using the DFTB3LYP/3-21G method in GAMESS software [40, 41]. Calculations were carried out only between the components, without applying any solvent effect.

The natural bond orbital (NBO) analysis is a useful tool for investigating the delocalization of electron density from occupied Lewis-type NBOs (act as a donor) to unoccupied non-Lewis type NBOs (act as acceptor) within a molecule or between two molecules. The stabilization of orbital interaction is related to the energy difference between the interacting orbitals. The strongest stabilizer interaction has been found between effective donors and acceptors. The interaction between bonding and anti-bonding molecular orbitals can be quantitatively described in terms of second-order perturbation interaction energy E (2). A larger E (2) (energy of hyperconjugative interactions) shows the more intensive interaction between electron donors and electron acceptors. In the formation of H-bonds process, a certain amount of electronic charge transfer occurs from the lone pairs of the proton acceptor to the anti-bonding orbitals of the proton donor molecule [42-45].

The structures of PVP dimer and a half monomer of PANI emeraldine salt were optimized, separately. Then, these structures were optimized together in order to obtain the most stable structure of two polymers. ZnO and TiO_2 nanoparticles were optimized as $(ZnO)_4$ and $(TiO_2)_3$, respectively, based on the structures optimized in the literature [46, 47]. These structures and SO_4^{2-}, Na^+, and Cl^- ions were optimized with two polymers under different situations in order to obtain the most stable structure. Eventually, the NBO analysis was implemented.

RESULTS AND DISCUSSION

Preparation

The particles of polyaniline aggregate in high concentrations. Therefore, distributions of the filler in the composite matrix were lost, leading to a decline in the mechanical properties of this composite [19]. As a result, the weight percentage of PANI was reduced in this study compared with those of other works [7, 11]. As mentioned in the literature, a low molecular weight PVP has poor mechanical properties [48] and thus a high molecular weight PVP was used during this study.

Mechanical Properties

The effects of TiO_2, ZnO, NaCl, and Na_2SO_4 on tensile strength, elongation at break and Young's modulus (*E*) of PVP/PANI films are presented in Fig. 1 and Table 1. Tensile strength results were obtained with the following order: PVP/PANI/TiO_2 > PVP/PANI/ZnO > PVP/PANI > PVP/PANI/Na_2SO_4 > PVP/PANI/NaCl. In comparison, the order of the strain was as: PVP/PANI > PVP/PANI/TiO_2 > PVP/PANI/ZnO > PVP/PANI/Na_2SO_4 > PVP/PANI/NaCl. Finally, the order of Young's modulus is similar to that of the tensile strength.

Addition of ZnO and TiO_2 leads to an increase in the PVP/PANI tensile strength and Young's modulus, but decrease the elongation at break. However, NaCl and Na_2SO_4 reduce strength, strain, and tensile modulus, suggesting that the nanoparticles modified the film resistance. It can be seen from Fig. 1 that nanomaterials increase the tensile strength while mineral salts decrease it. An increase in tensile strength and tensile modulus by ZnO and TiO_2 may be attributed to the good dispersion, strong interfacial adhesion between the nanomaterials and polymers; as can be seen from SEM [31] (via H-bonding interactions), occupied spaces between the polymeric chains by fillers, and improved rigidity of nanocomposites [18, 49]. The interaction of nanomaterials was established through its surface hydroxyl groups with polar parts of the polymers [50].

Table 1: Tensile strength, Elongation at break, and Young's modulus of PVP/PANI composites.

	Tensile strength (MPa)	Elongation at break (%)	Young 's modulus (MPa)
PVP/PANI	21.1	11.4	8.9
PVP/PANI /ZnO	25.2	9.8	9.5
PVP/PANI /TiO_2	27.9	10.2	11.1
PVP/PANI /NaCl	13.3	7.9	6.9
PVP/PANI /Na_2SO_4	18.7	9.3	7.8

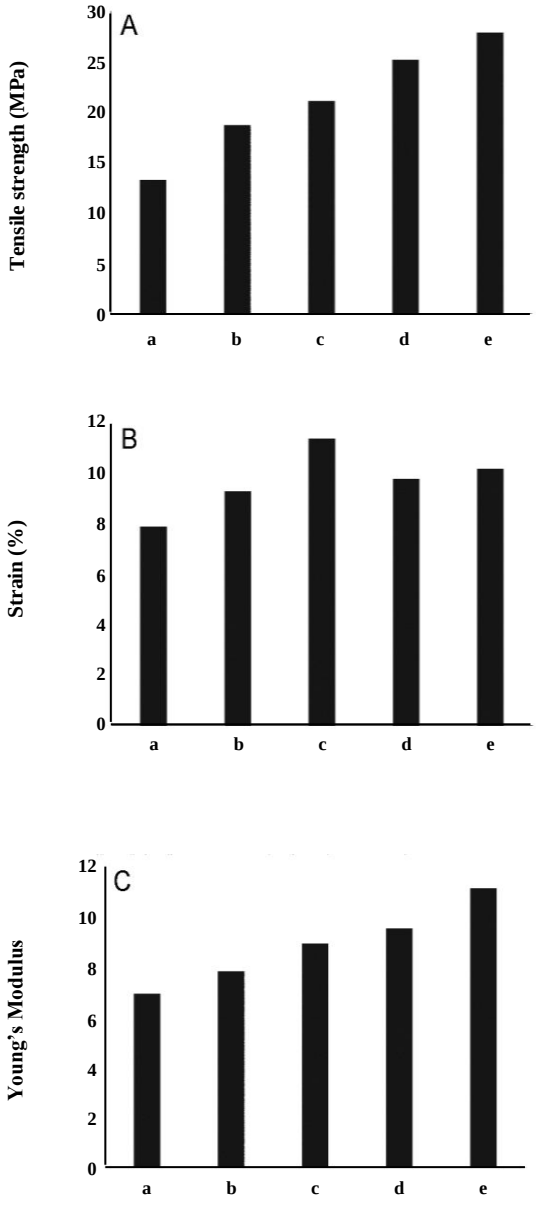

Fig. 1: (A) Tensile stress, (B) Tensile strain and (C) Young's modulus of (a) PVP/PANI/NaCl, (b) PVP/PANI/Na_2SO_4, (c) PVP/PANI, (d) PVP/PANI/ZnO, and (e) PVP/PANI/TiO_2.

As mentioned in literature, the aggregation of additives increases the elongation of films. However, the elongation at break is decreased by the compatibility of polymer-nonmaterial [51]. The elongation of the composite films decreases because of the rigid or brittle nature of nanoparticles and restriction of the ductile deformation of the polymer chains. These results show that TiO_2 and ZnO growth absorbed the energy by the matrix, throughout the deformation process [18]. Presumably, reduction in tensile strength and strain in PVP/PANI/NaCl and PVP/PANI/Na_2SO_4 is ascribed to the immiscibility due to their differences in polarity. This result led to a reduction in filler-polymer interaction, which weakened the interactions within the polymer network, which acts as the matrix of the composite films. The poor filler-polymer interaction induced growing the deformation of the matrix (caused by the energy dissipating), leading to the creation of weak points in the polymer matrix [31]. The small-sized dopant usually is colonized out of the polymer matrix. These results are in good agreement with other studies [49, 52].

According to Nand et al. and Barra et al. studies, reduction in tensile strength and Young's modulus showed that NaCl and Na_2SO_4 have a plasticizing effect [49, 53]. Reduction of the elongation at failure point showed that the film becomes more brittle [5, 52]. Fig. S1 illustrates the stress-strain curves. As can be seen, PVP/PANI/NaCl broke at lower strains, showing that it is hard and brittle, while the softest composite is PVP/PANI. These results imply the improved PANI processability by blending with a soluble polymer as a matrix [52]. A comparison between the results in Table S1 showed that the tensile strength is more sensitive to additives than the elongation at break.

Rheological measurement

The angular frequency versus G′ and G″ for all samples (at 1% strain amplitude) is shown in Fig. 2.

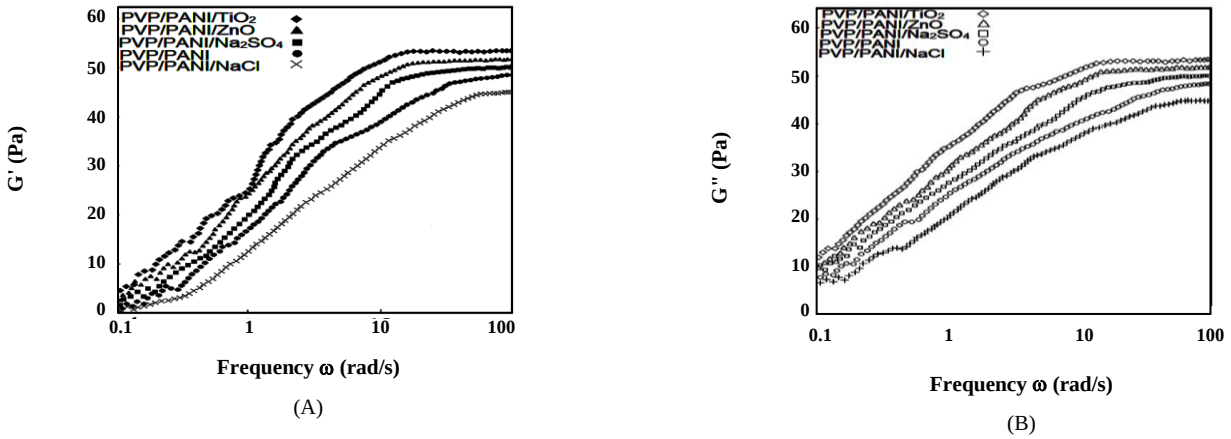

Fig. 2: The angular frequency dependency of (A) storage modulus (G') and (B) loss modulus (G") at 1% strain amplitude.

According to this figure, G′ and G″ increase sharply at higher frequencies, representing a transition from viscous to elastic behavior at a higher frequency, which is in good agreement with the literature [17]. Although G′ is low in the solution, it increases sharply when gelation is commenced [39].

The hydrogen bonding between the PVP and PANI causes the formation of a network-like structure [17], which can be responsible for elastic modulus increases. In comparison with chemical bonding, hydrogen bonding between the polymers is very weak, so this solution cannot transform to a gel. Elastic property is more sensitive than viscous property to hydrogen bonding in the system [17]. Therefore, G' is more affected by hydrogen bonding and can be used as a criterion for the evaluation of the hydrogen bonding in different systems.

From Fig. 2, it is apparent that G' and so interactions between components increase in PVP/PANI/Na_2SO_4 and PVP/PANI/ZnO, and maximized in PVP/PANI/TiO_2 in comparison with PVP/PANI. However, interactions between components come down in the presence of NaCl. Fig. 2a shows that the G' of PVP/PANI increased after the addition of Na_2SO_4, ZnO, and TiO_2. NaCl decreases the storage modulus. Accordingly, hydrodynamic interactions of the TiO_2 nanoparticles and the probability of collision increase, leading to the aggregation processes. Because of the interactions between TiO_2 and polymers (hydrogen bonding is most important), the polymer chains' mobility was restricted. Furthermore, this could be related to the stress transfer from the polymer matrix to the included particles and the reduction of polymer chain movement.

ZnO nanoparticles improve the matrix stiffness. This effect may be related to the increase in the crystallinity of the matrix, due to the strong filler-matrix interfacial adhesion. The latter is originated from hydrogen bonding between the OH groups of ZnO and the C=O and N in the PVP and PANI, respectively. This result is in good agreement with the literature [18]. Na_2SO_4 helps the formation of elastic gel when mixed with polymer solution systems. The rise in these moduli may be related to the strong interactions between salt ions and polymers. The addition of sulfate ions leads to forming a complex with water molecules that reduces the solvent species in the polymer chain environment and induce the aggregation of polymer chains, which lead to the gel formation. NaCl acts as a plasticizer and makes PVP/PANI softer [5]. The weakening of interchain interaction (hydrogen bonding) or crosslinking led to reducing the elastic property [17].

Fig. S2 represents the storage modulus and loss modulus. According to Fig. S2, G' is lower than G", suggesting that no strong hydrogel exists [39]. At higher frequency, a superposition of G' and G" is observable. Fig. 3 represents the complex viscosity versus angular frequency. During the synthesis of this blend, interactions (hydrogen bonds) were established between PVP and PANI chains and other additives. These interactions cause the formation of a network-like structure, which increases the viscosity of these blends. Fig. 3 shows that the viscosity was reduced in all samples, indicating a shear thinning behavior related to the induced chain orientation and reduction of the entanglement or weakly flocculated nature of the solutions [17, 35].

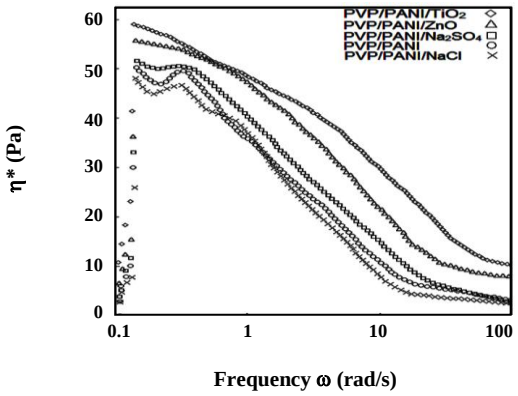

Fig. 3: The complex viscosity (η*) versus angular frequency (ω) of PVP/PANI composite

Moreover, a viscosity increase by TiO_2 may be attributed to an anisotropic particle microstructure formed at a steady shear, in accordance with other studies [54]. Furthermore, the rise in viscosity may be related to the strong interactions between salt ions and polymers in the PVP/PANI/Na_2SO_4 [29]. However, interactions between polymers are weakened by NaCl. With increasing angular frequency, the interpolymer network-like structure was crushed, leading to a shear-thinning behavior. When interactions (specifically hydrogen bonding in the systems) become stronger, viscosity shows an increase [17]. This behavior can be considered as a criterion for the power of the interactions between the system components. As can be seen from Fig. 3, viscosity and, therefore, the interactions between components increase in PVP/PANI/Na_2SO_4 and PVP/PANI/ZnO, respectively, and maximized in PVP/PANI/TiO_2.

NBO analysis

The hydrogen bonding between PVP and PANI were investigated theoretically and experimentally. The results show the hydrogen bonding between the acidic hydrogen atoms in PANI imine groups and the electronegative oxygen atoms in PVP carbonyl groups. The H-bonds lead to a high degree of dispersion and stability [1, 7]. In this study, NBO results were used for scrutiny of the interactions between additives (TiO_2, ZnO, Na^+, Cl^-, and SO_4^{2-}) and the two polymers (PVP and PANI). Dimer of PVP and half monomer of PANI Emeraldine salt were optimized separately. Then, PVP and PANI were optimized with together in order to obtain the most stable structure of two polymers (Fig. S3 [55]) and finally, the NBO analysis was implemented. SO_4^{2-} anion, TiO_2, and ZnO nanoparticles were optimized separately. Optimization of ZnO nanoparticle structure was implemented as $(ZnO)_4$ based on the study of *Cheng et al.* (Fig. S3) [46]. Similarly, optimization of TiO_2 nanoparticle structure was performed as $(TiO_2)_3$ based on the study of Pandey et al. (Fig. S3) [47]. Then, these structures and Na^+ and Cl^- ions were optimized with the structures of two polymers to obtain the most stable structure (Fig. S3), followed by implementing the NBO analysis.

The selected "second-order perturbation theory analysis of Fock Matrix" in NBO basis for PVP/PANI, PVP/PANI/Cl^-, PVP/PANI/Na^+, PVP/PANI/SO_4^{2-}, PVP/PANI/TiO_2, and PVP/PANI/ZnO are represented in Table S2 (only interactions between PVP and PANI represented). As its monomers [56], nitrogen atoms in PANI are important in the interaction of PANI with other chemical species. These results show the strong interaction between acidic hydrogen in PANI imine (H13) and the electronegative oxygen atom (O53) in the PVP carbonyl group. Furthermore, Table S2 shows the additives did not affect strongly the PVP and PANI interactions (except Cl^-). Chloride anions weakened the PVP-PANI interactions. Tables S3 to S7 exhibit the interactions between PVP/PANI and Cl^-, Na^+, SO_4^{2-}, TiO_2, and ZnO. Based on these tables, the strongest interactions occur between TiO_2 and PVP/PANI. The order of interactions between polymers and additives was as TiO_2 > ZnO > SO_4^{2-} > Cl^- > Na^+. These results show a good agreement with experimental results.

CONCLUSIONS

The tensile strength and the Young's modulus showed the order of PVP/PANI/TiO_2 > PVP/PANI/ZnO > PVP/PANI > PVP/PANI/Na_2SO_4 > PVP/PANI/NaCl while the strain order was PVP/PANI > PVP/PANI/TiO_2 > PVP/PANI/ZnO > PVP/PANI/Na_2SO_4 > PVP/PANI/NaCl. An increase in tensile strength and tensile modulus by ZnO and TiO_2 attributed to the strong interfacial adhesion between the nanomaterials and polymers. The compatibility between nanomaterials and polymer leads to a decrease in elongation at break. Reduction in tensile strength and strain by NaCl

and Na_2SO_4 is attributed to the poor filler-polymer interaction. The G' (and so, interactions between components) was seen in the order of PVP/PANI/TiO_2 > PVP/PANI/ZnO > PVP/PANI/Na_2SO_4 > PVP/PANI/NaCl. During the synthesis of this blend, a network-like structure was formed, which increased the viscosity. Interactions between polymers were weakened by NaCl. The viscosity and interactions between components increase by Na_2SO_4, ZnO, and maximized by TiO_2, respectively. The NBO results show that the additives did not affect strongly the PVP and PANI interactions (except Cl^-). Chloride anions reduced the interactions between PVP and PANI. The strongest interaction was seen between TiO_2 and PVP/PANI. Furthermore, ZnO, SO_4^{2-}, Cl^-, and Na^+ have strong interactions with PVP/PANI. All methods applied in this research represented that the interactions among components are in the following order: PVP/PANI/TiO_2 > PVP/PANI/ZnO > PVP/PANI/Na_2SO_4 > PVP/PANI/NaCl. Among these additives, TiO_2 and ZnO improved the mechanical properties of the PVP/PANI blend.

Conflict of Interests

The authors declare that there is no conflict of interest regarding the publication of this paper.

Received : Jul. 8, 2018 ; Accepted : Oct. 8, 2018

REFERENCES

[1] Tang J., Ma L., Huo Q., Yan J., Tian N., Xu F., The Influence of PVP on the Synthesis and Electromagnetic Properties of PANI/PVP/CIP Composites, *Polym. Compos.*, **36**: 1799-1806 (2015).

[2] Zhao S., Wang Z., Wei X., Zhao B., Wang J., Yang S., Wang S., Performance Improvement of Poly Sulfone Ultrafiltration Membrane Using Well-Dispersed Polyaniline-Poly (vinylpyrrolidone) Nanocomposite as the Additive, *Ind. Eng. Chem. Res.*, **51**: 4661-4672 (2012).

[3] Kajekar A.J., Dodamani B.M., Isloor A.M., Abdul Karim Z., Be Cheer N., Ismail A.F., Shilton S.J., Preparation and Characterization of Novel PSf/PVP/PANI-Nanofiber Nanocomposite Hollow Fiber Ultrafiltration Membranes and Their Possible Applications for Hazardous Dye Rejection, *Desalination*, **365**: 117-125 (2015).

[4] Faghihian H., Rasekh M., Removal of Chromate from Aqueous Solution by a Novel Clinoptilolite-Polyanillin Composite, *Iran. J. Chem. Chem. Eng. (IJCCE)*, **33:** 45-51 (2014).

[5] Jiang X., Jiang T., Gan L., Zhang X., Dai H., Zhang X., The Plasticizing Mechanism and Effect of Calcium Chloride on Starch/Poly(vinyl alcohol) Films, *Carbohydr. Polym.*, **90:** 1677-1684 (2012).

[6] Murugesan R., Anitha G., Subramanian E., Multi-faceted Role of Blended Poly vinylpyrrolidone Leading to Remarkable Improvement in Characteristics of Polyaniline Emeraldine Salt, *Mater. Chem. Phys.*, **85:** 184-194 (2004).

[7] Pan W., Qu L., Chen Y., Conductive Blends of Dodecylbenzen Sulfonic Acid Doped Polyaniline with Poly vinylpyrrolidone, *Optoelectron. Adv. Mat.*, **4:** 2123-2128 (2010).

[8] Bayandori Moghaddam A., Hosseini S., Badraghi J., Banaei A., Hybrid Nanocomposite Based on $CoFe_2O_4$ Magnetic Nanoparticles and Polyaniline, *Iran. J. Chem. Chem. Eng. (IJCCE)*, **29:** 173-179 (2010).

[9] Abdelrazek E.M., Ragab H.M., Abdelaziz M., Physical Characterization of Poly (vinyl pyrrolidone) and Gelatin Blend Films Doped with Magnesium Chloride, *Plast. Polym. Technol.*, **2:** 1-8 (2013).

[10] Subramanian E., Anitha G., Vijayakumar N., Constructive Modification of Conducting Polyaniline Characteristics in Unusual Proportion Through Nanomaterial Blend Formation with the Neutral Polymer Poly(vinyl pyrrolidone), *J. Appl. Polym. Sci.*, **106:** 673-683 (2007).

[11] Palaniappan S., Sairam M., Benzoyl Peroxide as a Novel Oxidizing Agent in Polyaniline Dispersion: Synthesis and Characterization of a Pure Polyaniline-Poly (vinyl pyrrolidone) Composite, *J. Appl. Polym. Sci.*, **108:** 825-832 (2008).

[12] Ates M., Kalender O., Comparison of Anticorrosion Behavior of Polyaniline and Poly (3,4-methylenedioxyaniline) and Their Titanium Dioxide Nanocomposites, *High. Perform. Polym.*, **27:** 685-693 (2015).

[13] Tang J., Ma L., Tian N., Gan M., Xu F., Zeng J., Tu Y., Synthesis and Electromagnetic Properties of PANI/PVP/CIP Core-Shell Composites, *Mater. Sci. Eng. B*, **186:** 26-32 (2014).

[14] Jafari Y., Ghoreishi S.M., Shabani Nooshabadi M., Electrosynthesis, Characterization and Corrosion Inhibition Study of DBSA-Doped Polyaniline Coating on 310 Stainless Steel, *Iran. J. Chem. Chem. Eng. (IJCCE)*, **36**: 23-32 (2017).

[15] Ghasemi M., Kowsari E., Amoozadeh A., Chitosan/Poly(Amide-Imide) Blend Films: Studies on Thermal and Mechanical Stability, Morphology and Biodegradability, *Iran. J. Chem. Chem. Eng. (IJCCE)*, **36**(2)**:** 55-70 (2017).

[16] Garai A., Nandi A.K., Rheology of (±)-Camphor-10-Sulfonic Acid Doped Polyaniline-m-Cresol Conducting Gel Nanocomposites, *J. Polym. Sci. Part. B Polym. Phys.*, **46:** 28-40 (2008).

[17] Gangopadhyay R., Exploring Rheological Properties of Aqueous Polyaniline-PVP Dispersion. *J. Polym. Sci. Part B Polym. Phys.*, **46:** 2443-2455 (2008).

[18] Diez-Pascual A.M., Diez-Vicente A.L., Poly(3-hydroxybutyrate)/ZnO Bionanocomposites with Improved Mechanical, Barrier and Antibacterial Properties. *Int. J. Mol. Sci.*, **15:** 10950-10973 (2014).

[19] Yilmaz F., "Polyaniline: Synthesis, Characterization, Solution Properties and Composites", PhD Thesis, Middle East Technical University: Turkey (2007).

[20] Abusaidi H., Ghaieni H., Ghorbani M., Influences of NCO/OH and triol/diol Ratios on the Mechanical Properties of Nitro-HTPB Based Polyurethane Elastomers, *Iran. J. Chem. Chem. Eng. (IJCCE)*, **36:** 55-63 (2017).

[21] Nikrarjam A., Salehifar N., Improvement In Gas-Sensing Properties of TiO_2 Nanofiber Sensor By UV Irradiation, *Sens. Actuators B*, **211:** 146-156 (2015).

[22] Wei J.H., Zhang Q., Liu Y., Xiong R., Pan C.X., Shi J., Synthesis and Photocatalytic Activity of Polyaniline-TiO_2 Composites with Bionic Nanopapilla Structure, *J. Nanopart. Res.*, **13:** 3157-3165 (2011).

[23] Khademian M., Eisazadeh H., Preparation and Characterization Emulsion of PANI-TiO_2 Nanocomposite and Its Application as Anticorrosive Coating, *J. Polym. Eng.*, **35:** 597-603 (2015).

[24] Patil P.T., Anwane R.S., Kondawar S.B., Development of Electrospun Polyaniline/ZnO Composite Nanofibers for LPG Sensing, *Procedia Mater. Sci.*, **10:** 195-204 (2015).

[25] Zieleniewska M., Auguscik M., Prociak A., Rojek P., Ryszkowska J., Polyurethane-Urea Substrates from Rapeseed Oil-Based Polyol for Bone Tissue Cultures Intended for Application in Tissue Engineering, *Polym. Degrad. Stab.*, **108:** 241-249 (2014).

[26] Lai C.Y., Groth A., Gray S., Duke M., Impact of Casting Conditions on PVDF/Nanoclay Nanocomposite Membrane Properties, *Chem. Eng. J.*, **267:** 73-85 (2015).

[27] Villoslada I.M., Hermosilla R.A., Fuenzalida J.P., Pizarro G. del C., Tripailaf G., Marambio O.G., Nishide H., Comparative Study of the Self-Aggregation of Rhodamine 6G in the Presence of Poly (sodium 4-styrenesulfonate), Poly (*N*-phenylmaleimide-*co*-acrylic acid), Poly (styrene-*alt*-maleic acid), and Poly(sodium acrylate), *J. Phys. Chem. B*, **114:** 11983-11992 (2010).

[28] Li J., Zhou M., Lin J.Y., Ye W.Y., Xu Y.Q., Shen J.N.J.N., Gao C.J., Van der Bruggen B., Monovalent Cation Selective Membranes for Electrodialysis by Introducing Polyquaternium-7 in a Commercial Cation Exchange Membrane, *J. Membr. Sci.*, **486:** 89-96 (2015).

[29] Yin W., Zhang H., Huang L., Nishinari K., Effects of the Lyotropic Series Salts on the Gelation of Konjacglucomannan in Aqueous Solutions, *Carbohydr. Polym.*, **74:** 68-78 (2008).

[30] Ananda H.T., Thejas Urs G., Somashekar R., Preparation and Characterization of Conductive PVA/Gly: Na_2SO_4 Polymer Composites, *Polym. Bull.*, **73:** 1151-1165 (2016).

[31] Taghizadeh M.T., Nasirianfar, Ultraviolet Irradiation Effect on Polyvinylpyrrolidone/Polyaniline Films with Additives, *Polym. Plast. Technol. Eng.*, 57: 1893 – 1905 (2018).
DOI: 10.1080/03602559.2018.1447124.

[32] Suknuntha K., Jones D.S., Tantishaiyakul V., Properties of Felodipine-Poly (vinyl pyrrolidone) Solid Dispersion Films and the Impact of Solvents, *Science Asia*, **38:** 188-195 (2012).

[33] da Silva M.J., Sanches A.O., Malmonge L.F., Malmonge J.A., Electrical, Mechanical, and Thermal Analysis of Natural Rubber/Polyaniline-Dbsa Composite, *Mater. Res.* (Suppl. 1), **17:** 59-63 (2014).

[34] Lobotka P., Kunzo P., Kovacova E., Vavra I., Krizanova Z., Smatko V., Stejskal J., Konyushenko E.N., Omastova M., Spitalsky Z., Micusik M., Krupa I., Thin Polyaniline and Polyaniline/Carbon Nanocomposite Films for Gas Sensing, *Thin Solid Films*, **519:** 4123-4127 (2011).

[35] Saengsuwan S., Bualek-Limcharoen S., Mitchell G.R., Olley R.H., Thermotropic Liquid Crystalline Polymer (Rodrun LC5000)/Polypropylene *in situ* Composite Films: Rheology, Morphology, Molecular Orientation and Tensile Properties, *Polymer*, **44**: 3407-3415 (2003).

[36] Djetoui Z., Djerboua F., Perena J., Benavente R., The Rheological Behavior of Wheat Starch Particulates Filled Uncured Styrene-Butadiene Rubber, *Iran. J. Chem. Chem. Eng. (IJCCE)*, **36**: 159-172 (2017).

[37] Ozgur Bora M., Coban O., Avcu E., Fidan S., Sınmazcelik T., The Effect of TiO_2 Filler Content on the Mechanical, Thermal, and Tribological Properties of TiO_2/PPS Composites, *Polym. Compos.*, **34**: 1591-1599 (2013).

[38] Wu A.Q., Guo L.J., Liu C.S., Jia E.G., Zhu Z.G., The Experimental Viscosity and Calculated Relative Viscosity of Liquid In–Sn Allcoys, *Physica B*, **392:** 323-326 (2007).

[39] Shi Y., Xiong D., Liu Y., Wang N., Zhao X., Swelling, Mechanical and Friction Properties of PVA/PVP Hydrogels after Swelling in Osmotic Pressure Solution, *Mater. Sci. Eng. C*, **65:** 172-180 (2016).

[40] Gordon M.S., Schmidt M.W. "Advances in Electronic Structure Theory: GAMESS a Decade Later, Theory and Applications of Computational Chemistry.", C.E. Dykstra, G. Frenking, K.S. Kim, G.E. Scuseria (Ed.), "*The First Forty Years"*, Elsevier: Amsterdam, 1166-1168 (2005).

[41] Granovsky A.A., PC Gamess Version 7.1.G. Available at: http://classic.chem.msu.su/gran/gamess/index.html (2009, accessed July 2016).

[42] Gil D.M., Tuttolomondo M.E., Altabef A.B., Vibrational Studies (FTIR and Raman), Conformational Analysis, NBO, HOMO–LUMO and Reactivity Descriptors of S-methyl Thiobutanoate, $CH_3CH_2CH_2C(O)SCH_3$, *Spectrochim. Acta Mol. Biomol. Spectrosc.*, **149:** 408-418 (2015).

[43] Hmuda S., Trisovic N., Rogan J., Poleti D., Vitnik Z., Vitnik V., Valentic N., Bozic B., Uscumlic G., New Derivatives of Hydantoin as Potential Antiproliferative Agents: Biological and Structural Characterization in Combination with Quantum Chemical Calculations, *Monatsh. Chem.*, **145**: 821-833 (2014).

[44] Makiabadi B., Kian H., The Hydrogen Bond Interactions in Glycine–Nitrosamine Complexes: A DFT Study, *Monatsh. Chem.*, **146**: 69-78 (2015).

[45] Pakiari A.H., Farrokhnia M., Theoretical Study of Heteroatom Resonance-Assisted Hydrogen Bond: Effect of Substituent on π-delocalization, *Iran. J. Chem. Chem. Eng. (IJCCE)*, **29**: 197-210 (2010).

[46] Cheng X.X., Li F., Zhao Y., A DFT Investigation on ZnO Clusters and Nanostructures, *THEOCHEM*, **894**: 121-127 (2009).

[47] Chabungbam S., Loh G.C., Sahariah M.B., Pal A.R., Pandey R., Atomic Level Understanding of Site-Specific Interactions in Polyaniline/TiO_2 Composite, *Chem. Phys. Lett.*, **645:** 144-149 (2016).

[48] Chen W., Wang C., Yan L., Huang L., Zhu X., Chen B., Sant H.J., Niu X., Zhu G., Yu K.N., Roy V.A.L., Gale B.K., Chen X., Improved Polyvinylpyrrolidone Microneedle Arrays with Non-stoichiometric Cyclodextrin, *J. Mater. Chem. B*, **2:** 1699-1705 (2014).

[49] Nand A.V., Ray S., Travas-Sejdic J., Kilmartin P.A., Characterization of Antioxidant Low Density Polyethylene/Polyaniline Blends Prepared *via* Extrusion, *Mater. Chem. Phys.*, **135**: 903-911 (2012).

[50] Devi R.R., Maji T.K., Effect of Nano-ZnO on Thermal, Mechanical, UV Stability, and Other Physical Properties of Wood Polymer Composites, *Ind. Eng. Chem. Res.*, **51:** 3870-3880 (2012).

[51] Xuyuan Ji M., Wang T., Guo L., Xiao J., Li Z., Zhang L., Deng Y., He N., Effect of Nanoscale-ZnO on the Mechanical Property and Biocompatibility of Electrospun Poly(L-lactide) Acid/Nanoscale-ZnO, *J. Biomed. Nanotechnol.*, **9:** 417-423 (2013).

[52] Thanpitcha T., Sirivat A., Jamieson A.M., Rujiravanit R., Preparation and Characterization of Polyaniline/Chitosan Blend Film, *Carbohydr. Polym.*, **64**: 560-568 (2006).

[53] Barra G.M.O., Matins R.R., Kafer K.A., Paniago R., Vasques C.T., Pires A.T.N., Thermoplastic Elastomer/Polyaniline Blends: Evaluation of Mechanical and Electromechanical Properties, *Polym. Test.*, **27**: 886-892 (2008).

[54] Cabaleiro D., Pastoriza-Gallego M.J., Gracia-Fernandez C., Pineiro M.M., Lugo L., Rheological and Volumetric Properties of TiO_2-Ethylene Glycol Nanofluids, *Nanoscale Res. Lett.*, **8:** 286(1-13) (2013).

[55] http://www.chemcraftprog.com (accessed October 2016).

[56] Mohajeri S., Noei M., Molaei N., Cyanogen, Methylacetylene, Hydroquinone, Ethylacetylene, Aniline, Pyrrole, and Ethanol Detection by Using BNNT: DFT Studies, *Iran. J. Chem. Chem. Eng. (IJCCE)*, **36:** 89-98 (2017).

Supplementary Materials

Table S1: Percentage differences in tensile strength, elongation at break and Young's modulus at composites in comparison with the PVP/PANI.

	Tensile strength (MPa)	Elongation at break (%)	Young 's modulus (MPa)
PVP/PANI	21.1	11.4	8.9
PVP/PANI/ZnO	19.43%	-14.04%	6.74%
PVP/PANI/TiO_2	32.23%	-10.53%	24.72%
PVP/PANI/NaCl	-36.97%	-30.70%	-22.47%
PVP/PANI/Na_2SO_4	-11.37%	-18.42%	-12.36%

Table S2: Selected second order perturbation theory analysis of Fock Matrix in NBO Basis for PVP/PANI, PVP/PANI/Cl, PVP/PANI/Na, PVP/PANI/SO_4, PVP/PANI/TiO_2, PVP/PANI/ZnO. Only interactions between PVP and PANI represented. The structures calculated by B3LYP/3-21G method. Only E (2) (kcal/mol) has been reported.

From unit 1 (PANI) to unit 2 (PVP)					
Donor NBO (i)	Acceptor NBO (j)	E(2)	Donor NBO (i)	Acceptor NBO (j)	E(2)
PVP/PANI			PVP/PANI/Cl		
BD (1) N12-H13	BD*(1) C38-H41	0.96	BD (1) N12-H13	BD*(1) C38-H41	0.87
LP (1) N12	BD*(1) C38-H41	1.32	LP (1) N12	BD*(1) C38-H41	1.21
PVP/PANI/Na			PVP/PANI/SO4		
BD (1) N12-H13	BD*(1) C38-H41	0.95	BD (1) N12-H13	BD*(1) C38-H41	0.95
LP (1) N12	BD*(1) C38-H41	1.41	LP (1) N12	BD*(1) C38-H41	1.33
PVP/PANI/TiO2			PVP/PANI/ZnO		
BD (1) N12-H13	BD*(1) C38-H41	0.95	BD (1) N12-H13	BD*(1) C38-H41	0.95
LP (1) N12	BD*(1) C38-H41	1.33	LP (1) N12	BD*(1) C38-H41	1.31
From unit 2 (PVP) to unit 1 (PANI)					
Donor NBO (i)	Acceptor NBO (j)	E(2)	Donor NBO (i)	Acceptor NBO (j)	E(2)
PVP/PANI			PVP/PANI/Cl		
BD (2) C46-O53	BD*(1) N12-H13	1.26	BD (2) C46 - O53	BD*(1) N12-H13	1.09
LP (1) O53	BD*(1) C3-H9	1.33	LP (1) O53	BD*(1) C3-H9	1.18
LP (1) O53	BD*(1) N12-H13	4.09	LP (1) O53	BD*(1) N12-H13	3.36
LP (2) O53	BD*(1) C3-H9	0.73	LP (2) O53	BD*(1) C3-H9	0.56
LP (2) O53	BD*(1) N12-H13	0.57	LP (2) O53	BD*(1) N12-H13	0.44
PVP/PANI/Na			PVP/PANI/SO4		
BD (2) C46-O53	BD*(1) N12-H13	1.39	BD (2) C46-O53	BD*(1) N12-H13	1.41
LP (1) O53	BD*(1) C3-H9	1.34	LP (1) O53	BD*(1) C3-H9	1.4
LP (1) O53	BD*(1) N12-H13	4.01	LP (1) O53	BD*(1) N12-H13	4.22
LP (2) O53	BD*(1) C3-H9	0.95	LP (2) O53	BD*(1) C3-H9	0.82
LP (2) O53	BD*(1) N12-H13	0.73	LP (2) O53	BD*(1) N12-H13	0.61
PVP/PANI/TiO2			PVP/PANI/ZnO		
BD (2) C46-O53	BD*(1) N12-H13	1.27	BD (2) C46-O53	BD*(1) N12-H13	1.31
LP (1) O53	BD*(1) C3-H9	1.41	LP (1) O53	BD*(1) C3-H9	1.42
LP (1) O53	BD*(1) N12-H13	4.06	LP (1) O53	BD*(1) N12-H13	3.89
LP (2) O53	BD*(1) C3-H9	0.78	LP (2) O53	BD*(1) C3-H9	0.84
LP (2) O53	BD*(1) N12-H13	0.56	LP (2) O53	BD*(1) N12-H13	0.58

Table S3: Selected second order perturbation theory analysis of Fock Matrix in NBO Basis for PVP/PANI/Cl⁻ calculated by B3LYP/3-21G method. Only E (2) (kcal/mol) has been reported.

Donor NBO (i)	Acceptor NBO (j)	E(2) kcal/mol	Donor NBO (i)	Acceptor NBO (j)	E(2) kcal/mol
From unit 5 (Cl) to unit 1 (PANI)			From unit 5 (Cl) to unit 2 (PVP)		
LP (1)Cl65	BD*(2) C4-N12	1.95	LP (1)Cl65	BD*(1) C38-H41	2.94
LP (3)Cl65	BD*(2) C4-N12	2.75	LP (2)Cl65	BD*(1) N36-C38	2.74
LP (4)Cl65	BD*(1) C4-N12	1.19	LP (3)Cl65	BD*(1) N36-C38	2.03
LP (4)Cl65	BD*(2) C4-N12	4.07	LP (3)Cl65	BD*(1) C38-H41	2.4
From unit 3 (Cl) to unit 2 (PVP)			From unit 4 (Cl) to unit 2 (PVP)		
LP (1)Cl63	BD*(1) C46-C49	1.38	LP (1)Cl64	BD*(1) C27-H29	3.47
LP (1)Cl63	BD*(1) C49-H59	2.42	LP (3)Cl64	BD*(1) C27-H29	3.58
LP (2)Cl63	BD*(1) C47-C49	1.2	LP (3)Cl64	BD*(1) C37-O52	1.65
LP (3)Cl63	BD*(1) C46-C49	3.7	LP (3)Cl64	BD*(2) C37-O52	2.87
LP (4)Cl63	BD*(1) C46-C49	4.6	LP (4)Cl64	BD*(1) C27-H29	4.69
LP (4)Cl63	BD*(1) C49-H51	0.86	LP (4)Cl64	BD*(2) C37-O52	2.67
LP (4)Cl63	BD*(1) C49-H59	4.2			

Table S4: Selected second order perturbation theory analysis of Fock Matrix in NBO Basis for PVP/PANI/Na⁺ calculated by B3LYP/3-21G method. Only E (2) (kcal/mol) has been reported.

Donor NBO (i)	Acceptor NBO (j)	E(2) kcal/mol	Donor NBO (i)	Acceptor NBO (j)	E(2) kcal/mol
From unit 1 (PANI) to unit 4 (Na)			From unit 1 (PANI) to unit 5 (Na)		
BD (1) C3-H9	LP*(1)Na64	0.64	BD (2) C3-C4	LP*(1)Na65	0.38
BD (2) C3-C4	LP*(1)Na64	0.76	LP (1) N12	LP*(1)Na65	2.95
From unit 2 (PVP) to unit 3 (Na)			From unit 2 (PVP) to unit 4 (Na)		
BD (2) C37-O52	LP*(1)Na63	0.17	BD (2) C46 -O53	LP*(1)Na64	0.24
LP (1) O52	LP*(1)Na63	1.86	LP (1) O53	LP*(1)Na64	0.93
LP (2) O52	LP*(1)Na63	2.07	LP (2) O53	LP*(1)Na64	1.32
From unit 2 (PVP) to unit 5 (Na)			From unit 4 (Na) to unit 1 (PANI)		
BD (1) C38-H41	LP*(1)Na65	0.57	CR (2)Na64	BD*(1) C3-H9	0.56
LP (1) O53	LP*(1)Na65	1.07	CR (4)Na64	BD*(1) C3-H9	0.65
From unit 4 (Na) to unit 2 (PVP)			From unit 5 (Na) to unit 2 (PVP)		
CR (2)Na64	BD*(1) C49-H51	0.34	CR (2)Na65	BD*(1) C38-H41	0.57
CR (5)Na64	BD*(1) C49-H51	0.22	CR (3)Na65	BD*(1) C40-H55	0.55

Table S5: Selected second order perturbation theory analysis of Fock Matrix in NBO Basis for PVP/PANI/SO_4^{2-} calculated by B3LYP/3-21G method. Only E (2) (kcal/mol) has been reported.

Donor NBO (i)	Acceptor NBO (j)	E(2) kcal/mol	Donor NBO (i)	Acceptor NBO (j)	E(2) kcal/mol
From unit 3 (SO4) to unit 1 (PANI)			From unit 2 (PVP) to unit 4 (SO4)		
LP (2) O64	BD*(2) C16-C19	0.5	BD (1) C33-H34	BD*(1) S68-O71	1.07
LP (3) O66	BD*(1) C16-H20	1.74	LP (2) O52	BD*(1) S68-O71	0.13
From unit 4 (SO4) to unit 2 (PVP)			From unit 3 (SO4) to unit 2 (PVP)		
LP (1) O71	BD*(1) C33-H34	4.4	LP (1) O64	BD*(1) C49-H59	2.94
LP (3) O71	BD*(1) C33-H34	5.15	LP (2) O64	BD*(1) C49-H59	1.22
LP (2) O72	BD*(1) C33-H35	1.91	From unit 2 (PVP) to unit 3 (SO4)		
			BD (1) C49-H59	BD*(1) S63-O64	0.85

Table S6: Selected second order perturbation theory analysis of Fock Matrix in NBO Basis for PVP/PANI/TiO_2 calculated by B3LYP/3-21G method. Only E (2) (kcal/mol) has been reported.

Donor NBO (i)	Acceptor NBO (j)	E(2) kcal/mol	Donor NBO (i)	Acceptor NBO (j)	E(2) kcal/mol
From unit 1 (PANI) to unit 3 (Ti3O6)			From unit 1 (PANI) to unit 4 (Ti3O6)		
BD (1) C17-H22	BD*(1)Ti63-O64	1.91	BD (1) C2-H8	BD*(1)Ti72-O73	2.2
BD (1) C17-H22	BD*(2)Ti63-O64	1.86	BD (1) C3-H9	BD*(1)Ti77-O79	1.25
BD (1) C17-H22	BD*(1) O65-Ti67	2.5	BD (1) C3-H9	BD*(3)Ti77-O79	1.64
LP (1) N24	BD*(2)Ti63-O64	0.36			
LP (1) N24	BD*(2)Ti63-O66	0.38			
From unit 4 (Ti3O6) to unit 1 (PANI)			From unit 3 (Ti3O6) to unit 1 (PANI)		
BD (2)Ti72-O73	BD*(1) C2-H8	2.24	BD (2)Ti63-O64	BD*(1) N24-H26	4.7
BD (1)Ti77-O79	BD*(1) C3-H9	2.54	BD (1)Ti63-O65	BD*(1) C17-H22	4.63
BD (2)Ti77-O79	BD*(1) C3-C4	0.28	BD (2)Ti63-O66	BD*(1) N24-H26	2.1
BD (2)Ti77-O79	BD*(1) C3-H9	1.4	BD (3)Ti63-O66	BD*(2) C15-C17	0.76
LP (1) O73	BD*(1) C2-H8	6.42	BD (1) O65-Ti67	BD*(1) C17-H22	3.67
LP (2) O73	BD*(1) C2-H8	4.35	CR (3)Ti63	BD*(1) C17-H22	0.89
LP (1) O79	BD*(1) C3-C4	0.18	CR (5)Ti63	BD*(1) C17-H22	0.72
LP (1) O79	BD*(1) C3-H9	4.49	LP (1) O64	BD*(1) N24-H26	1.42
			LP (1) O65	BD*(1) C17-H22	6.24
			LP (1) O71	BD*(1) C17-H22	0.73
			LP (1) O71	BD*(1) N24-H26	0.62
From unit 3 (Ti3O6) to unit 2 (PVP)			From unit 4 (Ti3O6) to unit 2 (PVP)		
BD (2)Ti63-O66	BD*(1) C27-H28	1.07	BD (2)Ti77-O79	BD*(1) C38-H56	1.12
LP (1) O65	BD*(1) C27-H30	2.05	LP (1) O79	BD*(1) C38-H56	2.21
LP (2) O65	BD*(1) C27-H30	1.25			

Table S7: Selected second order perturbation theory analysis of Fock Matrix in NBO Basis for PVP/PANI/ZnO calculated by B3LYP/3-21G method. Only E (2) (kcal/mol) has been reported.

Donor NBO (i)	Acceptor NBO (j)	E(2) kcal/mol	Donor NBO (i)	Acceptor NBO (j)	E(2) kcal/mol
From unit 1 (PANI) to unit 3 (Zn4O4)			From unit 2 (PVP) to unit 3 (Zn4O4)		
BD (1) C2-H8	LP*(6)Zn63	2.17	BD (2) C46-O53	LP*(6)Zn67	3.25
BD (1) C3-H9	LP*(6)Zn63	1.96	BD (1) C49-H51	LP*(6)Zn67	1.63
			LP (1) O53	LP*(6)Zn67	5.22
			LP (2) O53	LP*(6)Zn67	0.99
			From unit 2 (PVP) to unit 4 (Zn4O4)		
			BD (1) C27-H28	LP*(6)Zn73	0.95
			BD (1) C27-H29	LP*(6)Zn73	1.32
From unit 3 (Zn4O4) to unit 1 (PANI)			From unit 3 (Zn4O4) to unit 2 (PVP)		
CR (2)Zn63	BD*(1) C2-H8	0.37	CR (3)Zn67	BD*(2) C46-O53	1.39
CR (3)Zn63	BD*(1) C2-H8	1.93	LP (1) O66	BD*(1) C49-H51	2.18
LP (1) O64	BD*(1) C2-H8	3.24	LP (2) O66	BD*(1) C49-H51	1.12
LP (2) O64	BD*(1) C3-H9	1.55	LP (1) O68	BD*(1) C49-H51	2.69
LP (1) O66	BD*(1) C2-H8	1.36	LP (2) O68	BD*(1) C46-O53	0.84
LP (2) O66	BD*(1) C2-H8	0.81	LP (1) O70	BD*(1) C49-H51	1.64
LP (1) O70	BD*(1) C3-H9	1.29	LP (2) O70	BD*(1) C49-H51	3.9
LP (2) O70	BD*(1) C2-H8	0.36			
LP (2) O70	BD*(1) C3-H9	2.5			
From unit 4 (Zn4O4) to unit 1 (PANI)			From unit 4 (Zn4O4) to unit 2 (PVP)		
LP (1) O72	BD*(1) C17-H22	2.21	LP (1) O72	BD*(1) C27-H30	2.26
LP (2) O72	BD*(1) C17-H22	1.22	LP (2) O72	BD*(1) C27-H30	1.58
			LP (1) O72	BD*(1) C27-H28	1.15

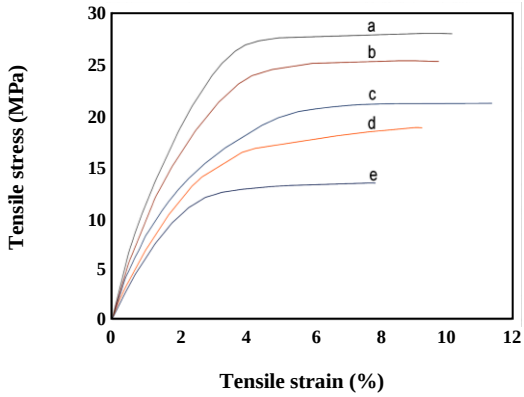

Fig. S1: Tensile Stress-Strain curves of (1) PVP/PANI/TiO_2 (2) PVP/PANI/ZnO (3) PVP/PANI (4) PVP/PANI/Na_2SO_4 and (5) PVP/PANI/NaCl.

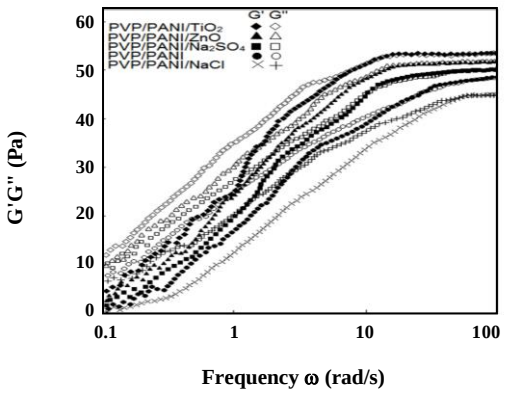

Fig. S2: The angular frequency (ω) dependency of storage modulus (G') and loss modulus (G") at 1% strain amplitude.

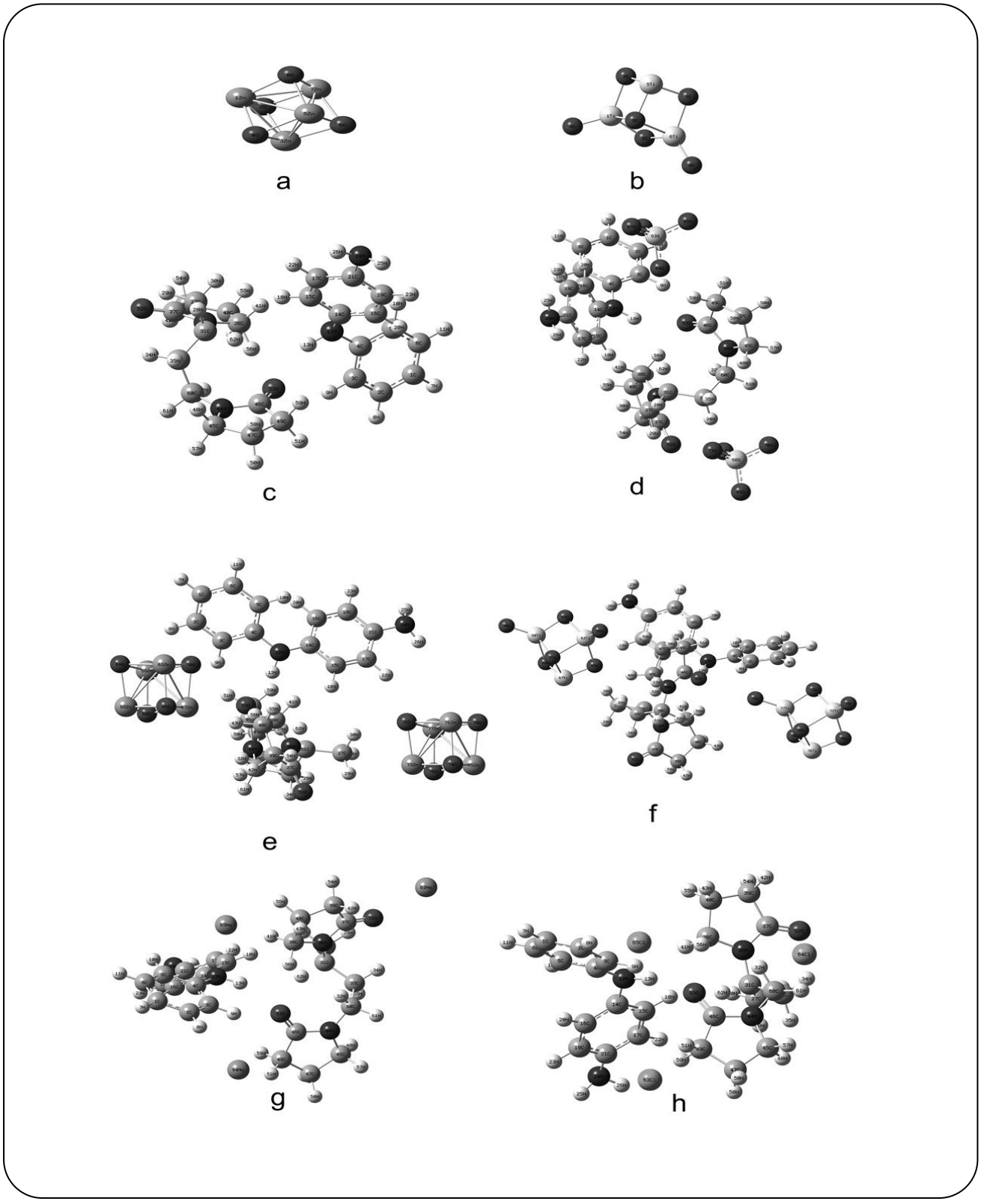

Fig. S3: Optimized structure of (a) $(ZnO)_4$ for ZnO nanoparticle, (b) $(TiO_2)_3$ for TiO_2 nanoparticle, (c) dimer of PVP and half monomer of PANI emeraldine salt, (d) PVP/PANI/SO_4^{2-}, (e) PVP/PANI/ZnO, (f) PVP/PANI/TiO_2, (g) PVP/PANI/Na^+, and (h) PVP/PANI/Cl^- were calculated by DFTB3LYP/3-21G.